Available online at www.sciencedirect.com
SCIENCE DIRECT®
Journal of Sound and Vibration 269 (2004) 197–211
JOURNAL OF SOUND AND VIBRATION
www.elsevier.com/locate/jsvi

Mitigation of chatter instabilities in milling by active structural control

Jeffrey L. Dohner[a,*], James P. Lauffer[a], Terry D. Hinnerichs[a], Natarajan Shankar[b], Mark Regelbrugge[c], Chi-Man Kwan[d], Roger Xu[d], Bill Winterbauer[e], Keith Bridger[f]

[a] *Sandia National Laboratories, Dept. 9234, Mailstop 0439, P.O. Box 5800, Albuquerque, NM 87185, USA*
[b] *Lockheed Martin Space Systems Company, 3251 Hanover St., Palo Alto, CA 94304, USA*
[c] *Rhombus Consultants Group, Inc., 2565 Leghorn St., Mountain View, CA 94043, USA*
[d] *Intelligent Automation, Inc., 2 Research Place, Suite 202, Rockville, MD 20850, USA*
[e] *Ingersoll Milling Machine Company, 707 Fulton Avenue, Rockford, IL 61103, USA*
[f] *Active Signal Technology, Inc., 13027-A Beaver Dam Road, Cockeysville, MD 21030, USA*

Received 10 October 2001; accepted 14 December 2002

Abstract

This paper documents the experimental validation of an active control approach for mitigating chatter in milling. To the authors knowledge, this is the first successful hardware demonstration of this approach. This approach is very different from many existing approaches that avoid instabilities by varying process parameters to seek regions of stability or by altering the regenerative process. In this approach, the stability lobes of the machine and tool are actively raised. This allows for machining at spindle speeds that are more representative of those used in existing machine tools.

An active control system was implemented using actuators and sensors surrounding a spindle and tool. Due to the complexity of controlling from a stationary co-ordinate system and sensing from a rotating system, a telemetry system was used to transfer structural vibration data from the tool to a control processor. Closed-loop experiments produced up to an order of magnitude improvement in metal removal rate.

1. Introduction

The following is a discussion of the experimental validation of an approach to enhance the productive capacity of a milling machine. This approach employs the use of active structural

*Corresponding author. Tel.: +1-505-844-5757; fax: +1-505-844-2991.
E-mail address: jldohne@sandia.gov (J.L. Dohner).

0022-460X/03/$ - see front matter © 2003 Elsevier Ltd. All rights reserved.
doi:10.1016/S0022-460X(03)00069-5

control technology to increase the performance of a machine by enhancing the stability of the cutting process. Unlike previous work, in this approach, the stability limits of the machine are altered. This approach was originally presented in 1997 in the paper by Dohner et al. [1], and, to the authors' knowledge, the following describes its first successful hardware implementation.

Maximum metal removal rate (MMRR) is a quantitative measure of the productive capacity of a machine tool. MMRR is limited by several factors including the onset of machining instabilities that are a function of the vibratory modes of both the machine and the tool [2–4]. By altering the dynamic characteristics of these modes, instabilities could be mitigated and MMRR improved. This alteration could be achieved by physically modifying the structure of a machine; however, this would be very costly and time consuming.

Many researchers have developed methods to *avoid* these instabilities by seeking regions of exiting stability [5,6]. Although promising for the high-speed machining of materials such as aluminum, for many ordinary materials, these approaches require running at speeds where tool wear can be excessive. To better illustrate this, consider Fig. 1, an illustration of the stability limits of a typical machine tool. As shown in this figure, lobbing effects produce regions of high stability in many machine tools. These lobes can be used to eliminate chatter by operating within a lobe. Nevertheless, most machines are not designed to operate at these speeds. Machines are designed to operate in a more confined section of the curve between η_{min} and η_{max} [ANSI/ASME standards]. In the approach described in this paper, it is assumed that the machine is designed to operate within this limited practical range.

Other approaches have been shown to mitigate chatter by varying spindle speed [7] or by modifying the periodicity of inserts within a tool. A cutting tool can have a number of inserts. As an insert cuts through metal it lays down a pattern, and this pattern affects the cut of the next insert on the tool. This interaction creates a dynamic feedback path between successive cuts, and, as in many feedback systems, can lead to instability. During cutting, energy is pumped into well coupled modes. If this energy pumping is great enough, energy gain will not be balanced by energy loss, and energy storage will grow; thereby, producing the dynamic instability known as

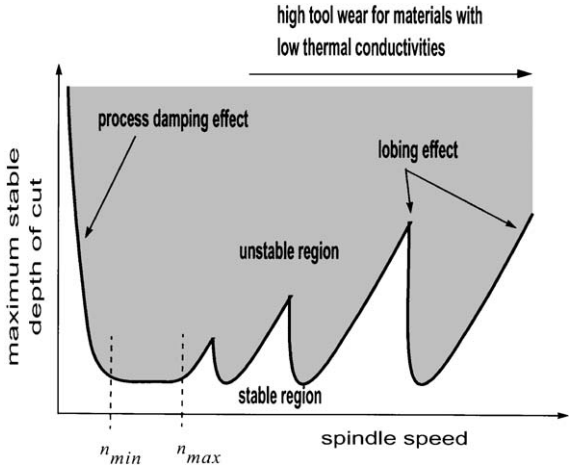

Fig. 1. Stability limits of a typical machine tool.

regenerative chatter. Varying spindle speed or changing the period of inserts on the tool can *modify* this pattern and limit the flow of energy into the tool. Nevertheless, many machine tools are not designed to operate in such a mode, and the modification of a large set of machine tools can be very expensive.

An alternative approach would be to use an active structural control system to alter dynamics. By properly altering these dynamics, the stability lobes of the machine and tool (i.e. maximum depth of cut vs. r.p.m. as shown in Fig. 1) will increase. This is very different from previous approaches that *avoid* instabilities by varying process parameters to seek regions of stability [5,6] or by altering the regenerative process [7]. Papers that discuss methods of avoiding instability are numerous, however, papers that discuss the use of active methods to improve stability, are relatively few [8–13], and almost all of these address turning, not milling. Moreover, the difficulties of performing active control in milling are far greater than those in turning where actuators and sensors can be located in the same stationary co-ordinate system.

The goal of the approach described herein is to ultimately develop a chatter suppression system that could be used on a wide variety of machines and machine tools. This is similar to the approach presented in Ref. [12] where an adaptive tool holder was constructed for the purpose of mitigating chatter instabilities. Although conceptionally successful, presented experimental results showed little of the periodic character of chatter, and therefore, a demonstration of performance improvements due to control were questionable at best.

The following sections present a hardware implementation of the theoretical approach presented in the paper by Dohner et al. [1]. Chatter suppression is performed by using an active control system to drive up the stability limits of a machine and tool. The chatter response presented in this paper shows itself as a strong instability in a mode of vibration. By using active control to limit this instability, up to an order of magnitude improvement in cutting performance was achieved.

2. Hardware design

An illustration of the hardware designed and constructed to demonstrate the utility of active control is shown in Fig. 2. Vibration is sensed at the root of a rotating tool by strain gages that are arranged in half bridge configurations to sense bending in two lateral directions. Excitation voltages were supplied to the half bridges using commercial electronics. Power is supplied to these electronics via magnetic coupling between rotating and stationary wires, and a telemetry system is used to transmit strain data from the rotating spindle to stationary receivers [14].

Strain is measured in a co-ordinate system that rotates with the shaft, (x, y, z), however, actuation occurs in a co-ordinate system that is stationary with the machine (X, Y, Z). Therefore, strain data must be translated from rotating to stationary co-ordinates. To do this, the angular position of the spindle is measured using a decoder. Decoder and strain-gage-bridge voltages are fed into anti-aliasing filters, analog-to-digital converters (A/D), and a processor for the computation of this transformation.

The anti-aliasing filters, the A/Ds, and the processor are part of a component called a controller. The controller captures voltage signals, combines them in accordance with a defined mathematical relationship, and outputs the result as another set of voltage signals. The defined

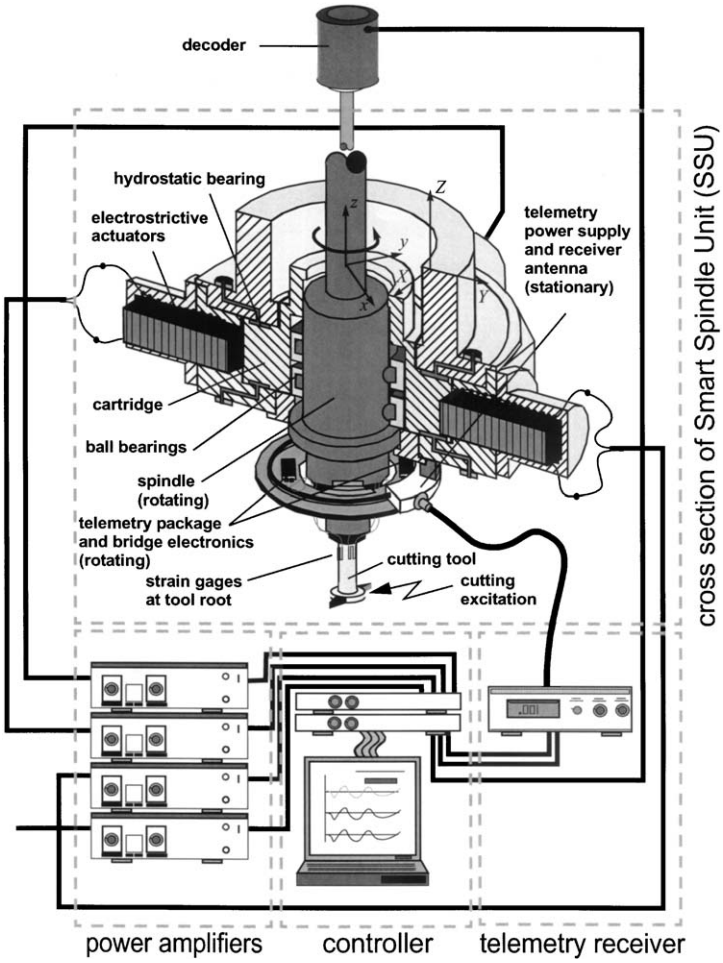

Fig. 2. Hardware configuration.

mathematical relationship is called a control law. As discussed below, control laws were designed to absorb energy from the rotating tool thereby, reducing entrapped energy. This absorption of energy increases the stability of the cutting process and improves MMRR.

As shown in Fig. 2, the controller produces four voltage signals that drive a set of four power amplifiers. These power amplifiers drive stacks of electrostrictive material (PMN) embedded within the housing of the machine. These stacks produce force against a non-rotating portion of the machine called the cartridge. The rotating spindle moves with the centerline of the cartridge. Thus, a force on the cartridge will produce motion in the tool. Motion corresponding to tool bending can be sensed by the strain gages and then fed back into the closed-loop control system.

Hardware, consisting of the spindle, the tool holder, the cartridge, the actuators, part of the telemetry system, and much of the surrounding housing were given the special name—the Smart Spindle Unit (SSU). A photograph of the SSU is shown in Fig. 3. Separate from the SSU are the power amplifiers, the controller, and the telemetry package receiver.

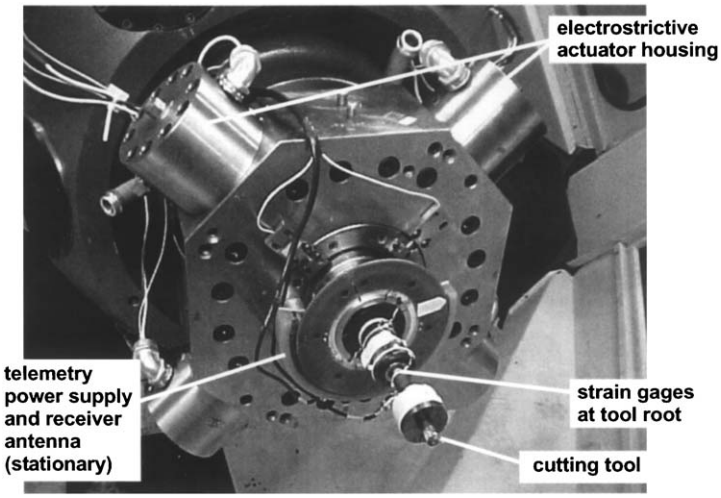

Fig. 3. Modified tool and smart spindle unit.

3. Characterization

Without the benefit of previous design data, the SSU design relied heavily on the use of numerical analysis [1]. Although this allowed for enough insight to complete an initial design, a full characterization of dynamics was required upon fabrication.

Initial experimental analysis of the SSU showed that system dynamics were not controllable or observable [15]. Frequency Response Functions (FRFs) were measured between voltage inputs to power amplifiers and tool strain responses in stationary co-ordinates. Initial measurements were made with the spindle at rest (0 r.p.m.). Fig. 4, is a plot of the maximum singular values (MSVs) of these FRFs. The MSVs give a bound of the FRF response of the system. Although, the first "tool" mode occurred at about 800 Hz, as shown in this figure, it did not participate in this response. Thus, a state-space model derived from measured FRFs would not contain the tool mode, and therefore, the tool mode could not be controlled or observed by a controller derived from this system model.

The reason the system was neither controllable nor observable was because of an anti-resonance in the FRFs. The frequency of the anti-resonance occurred at virtually the same frequency as the fundamental mode of the tool. The anti-resonance was due to modal cancellation between rigid-body modes of the cartridge/spindle system. Controllability and observability could have been achieved by shifting the resonant frequencies of the cartridge and spindle to frequencies above the fundamental frequency of the tool; however, to do this would have required a complete redesign of the SSU, and such modifications were beyond available budget.

Therefore, a mass was added close to the end of the existing tool to move the fundamental tool mode away from any anti-resonance. Subsequent FRFs are shown in Fig. 4. As shown, the tool mode (now clearly visible) was shifted from 800 Hz down to 453 Hz. The resulting realization (state-space model) of the modified system was both controllable and observable.

Additional measurements were performed to determine how FRFs varied with rotation. In Fig. 5, the maximum singular value of the actuator to strain FRFs for both rotating (3000 r.p.m.)

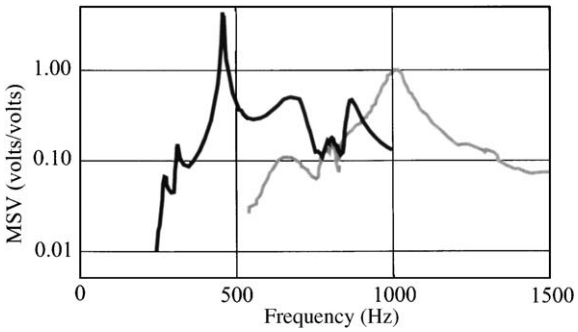

Fig. 4. Maximum singular value of FRFs showing the location of the tool mode: ——, unmodified system; ——, modified system.

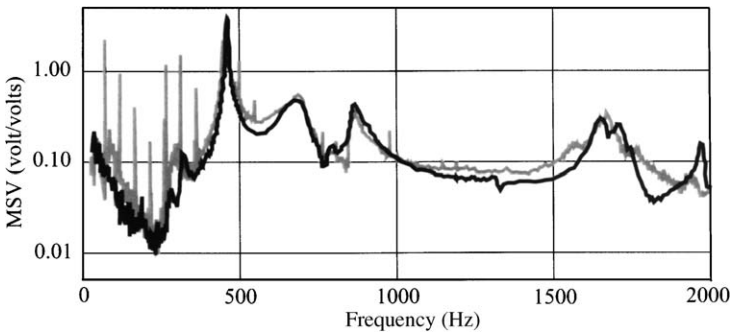

Fig. 5. Maximum singular value of FRFs for rotating and stationary spindles: ——, rotating spindle; ——, stationary spindle.

and stationary conditions are shown. The main difference between these plots is the presence of harmonics at multiples of the rotational speed of the spindle. These harmonics are artifacts due to bearing inputs, out-of-roundness, and balancing that could have been reduced by using more ensemble averages when estimating the FRFs. More importantly, Fig. 5 shows that the dynamics of the fundamental mode appears to be invariant with respect to rotation speed. Therefore, the same control law could be used regardless of spindle speed. This was an important fact that allowed for the use of the control design given below. It was expected considering that the maximum rotational frequency of excitation was only 4000 r.p.m. (67 Hz) whereas the modal instability occurred at 450 Hz, and the low-frequency system response was very low in amplitude. Thus, excitation due to spindle rotation did not significantly affect the response of the mode in question.

4. Control design

Control design was performed as a two-step process: (1) the production of a reduced order realization of dynamics, and (2) the design of a robust controller.

Fig. 6 shows controller logic. Three voltage signals are fed into the controller—two voltage signals from the receiver and a voltage signal from the decoder. These signals are passed through anti-aliasing filters and are then sampled. The result is a numerical data train representing tool strain, in rotating co-ordinates (x, y, z). These data are combined to calculate tool strain in the stationary co-ordinate system (X, Y, Z) (as discussed above).

At sample time k, stationary strain data is given in vector form by

$$\vec{y}(k) = \begin{bmatrix} \varepsilon_X(k) \\ \varepsilon_Y(k) \end{bmatrix},$$

where $\varepsilon_X(k)$ and $\varepsilon_Y(k)$ are sampled, stationary, strain data in the X and Y planes. This vector is used by the control law to compute the outputs of the controller. The control law takes the form

$$\vec{x}_c(k+1) = \boldsymbol{A}_c \vec{x}_c(k) + \boldsymbol{B}_c \vec{y}(k), \qquad \vec{u}(k) = \boldsymbol{C}_c \vec{x}_c(k), \tag{1a, b}$$

where $\boldsymbol{A}_c \in \Re^{n\times n}$ is the controller state matrix, $\boldsymbol{B}_c \in \Re^{n\times 2}$ is the controller input matrix, $\boldsymbol{C}_c \in \Re^{2\times n}$ is the controller output matrix, and n is the number of states in the controller [15]. For this application, the control law was designed to absorb energy from the system.

Using the control law and the data train, $\vec{y}(k), \vec{y}(k-1), \vec{y}(k-2), \ldots$, the output vector,

$$\vec{u}(k) = \begin{bmatrix} u_1(k) \\ u_2(k) \end{bmatrix},$$

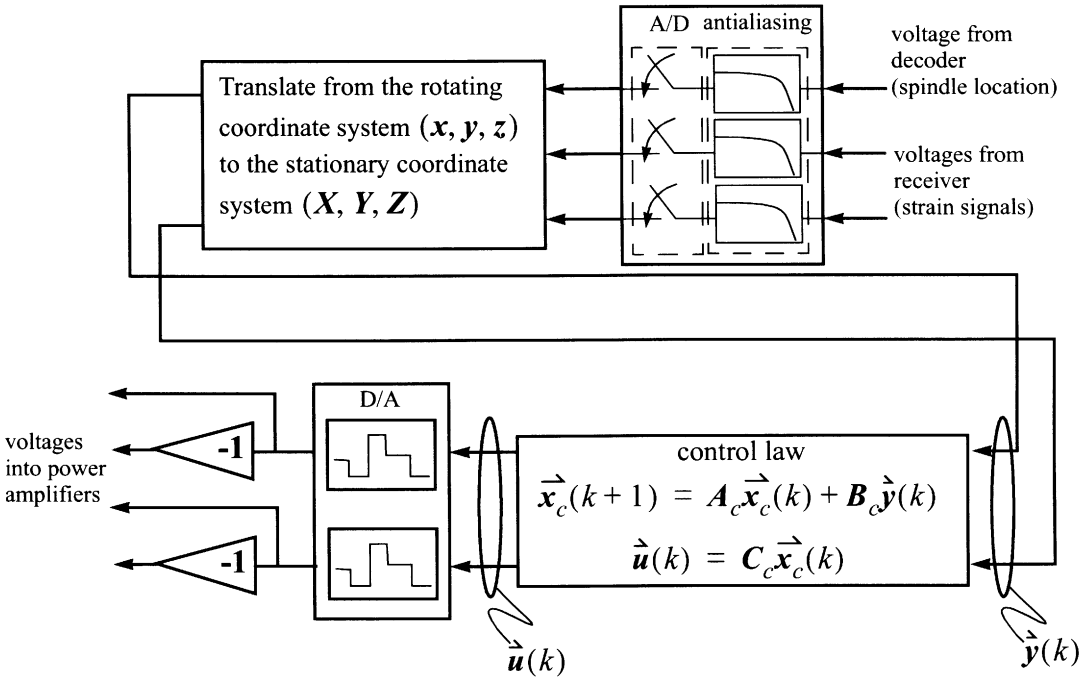

Fig. 6. Controller function in block diagram form.

can be calculated. The output vector data train is converted into two analog voltage signals by a set of digital-to-analog converters (D/A). Because of the cruciform configuration of the SSU, actuators on either side of the cartridge were assumed to move the same amount; therefore, voltage signals into the power amplifiers can be formed by splitting each D/A output voltage and changing the sign on one of the signals.

In order to choose a controller state, input, and output matrix that will damp tool motion, a mathematical realization of dynamics from $\vec{\boldsymbol{u}}(k)$ to $\vec{\boldsymbol{y}}(k)$ must be produced. This realization is often referred to as the plant. A variety of algorithms can be used to produce a plant realization from measured frequency response functions. The algorithm used in this effort was the Eigensystem Realization Algorithm with Direct Correlations, ERA/DC [16]. Neglecting any direct feed through effects, this algorithm produces a realization of the form

$$\vec{\boldsymbol{x}}(k+1) = \boldsymbol{A}\,\vec{\boldsymbol{x}}(k) + \boldsymbol{B}\,\vec{\boldsymbol{u}}(k), \qquad \vec{\boldsymbol{y}}(k) = \boldsymbol{C}\,\vec{\boldsymbol{x}}(k), \tag{2a, b}$$

where $\boldsymbol{A} \in \Re^{n\times n}$ is the plant state matrix, $\boldsymbol{B} \in \Re^{n\times 2}$ is the plant input matrix, and $\boldsymbol{C} \in \Re^{2\times n}$ is the plant output matrix. Again, n is the number of states.

The control law, Eq. (1a,b), is a mathematical relationship from $\vec{\boldsymbol{y}}(k)$ to $\vec{\boldsymbol{u}}(k)$. The plant, Eq. (2a,b), is a mathematical relationship from $\vec{\boldsymbol{u}}(k)$ to $\vec{\boldsymbol{y}}(k)$. Initially, a linear quadratic Gaussian (LQG) approach [15] was used to determine the state, input and output matrices of the control law. As with most practical uses of LQG, the weighting matrices used to define performance were manipulated to shape the loop until a sufficient balance between performance and robustness was achieved. Surprisingly, in doing this, it was found that LQG produced high levels of both robustness and performance. This occurred even for low order plant realizations ($n = 4$). After examination of the control law and plant, a better understanding of control dynamics was developed. Fig. 7 shows a Bode plot of the plant with and without control. Notice that there is one dominant mode in this system at 450 Hz. This is the tool mode. This tool mode has a peak response that is almost an order of magnitude greater than the response of any other mode in the

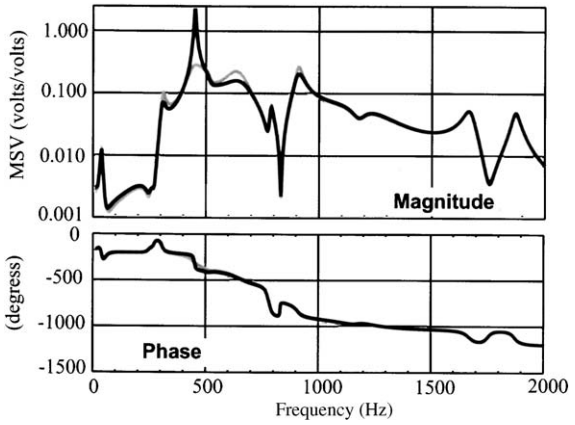

Fig. 7. Frequency response function, magnitude and phase, with and without control: ——, uncontrolled response; ——, controlled response.

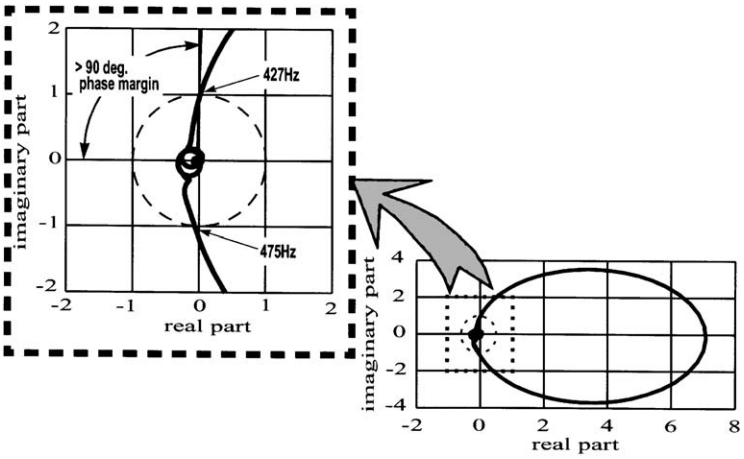

Fig. 8. Nyquist diagram of loop gain. Notice: the loop gain is greater than 1.0 only for frequencies around the fundamental tool frequency.

system. Therefore, the plant can be approximated as a second order system cascaded with all pass dynamics [17]. Considering symmetry and neglecting cross coupling, the plant can be approximated by

$$H(s) = \boldsymbol{C}(Is - \boldsymbol{A})^{-1}\boldsymbol{B} = \begin{bmatrix} \Gamma(s) & 0 \\ 0 & \Gamma(s) \end{bmatrix},$$

where $\Gamma(s) = \phi(s)K_s/(s^2 + 2\zeta\omega_n s + \omega_n^2), |\phi(s)| = 1$ and s is the Laplace transform variable. Numerical values for a 45th order plant realization (i.e. A, B, C) have been supplied in Appendix A.

The LQG approach produced controllers that can be approximated by

$$G_{(s)} = \boldsymbol{C}_c(Is - \boldsymbol{A}_c)^{-1}\boldsymbol{B}_c = \begin{bmatrix} \Theta(s) & 0 \\ 0 & \Theta(s) \end{bmatrix},$$

where $\Theta(s) = (K_c s + \alpha)/(s^2 + 2\zeta_c\omega_c \boldsymbol{s} + \omega_c^2)$. Notice that for $\omega \approx \omega_c$ and moderate values of K_s and K_c the loop gain, $\Theta(s)\Gamma(s)$, is greater than 1.0 only for frequencies near to ω. At all other frequencies the closed-loop system is gain stabilized. This has a significant influence on the Nyquist diagram of the loop gain. Fig. 8 shows the Nyquist diagram of the loop gain for a typical control law. The Nyquist diagram contains a single lobe that occurs near the fundamental frequency of the tool. The rotation and size of this lobe is controlled by the parameters K_c, ζ_c, and α. LQG selects these parameters such that the lobe is always deep in the right-hand plane of the Nyquist diagram. This gives high loop gains and therefore good performance while also maintaining robustness. Typical values for the controller have been supplied in Appendix A.

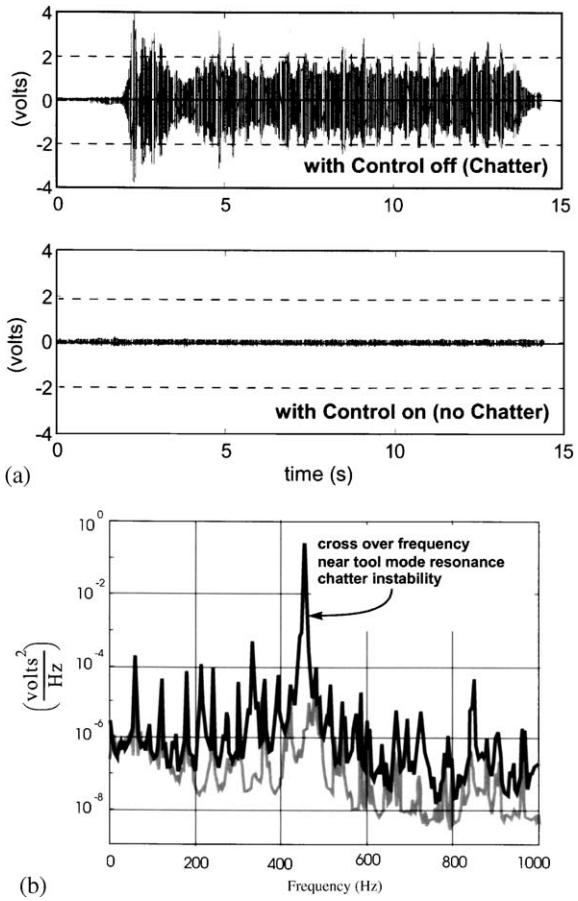

Fig. 9. (a) Unstable and stable dynamic response (time domain), strain response for a 0.01 mm depth of cut at 3600 r.p.m.; (b) power spectral densities of unstable and stable dynamic responses shown in Fig. 8(a); ——, with control off; ——, with control on.

5. Results

As discussed in the introduction, Fig. 1 is an illustration of the stability limits of a hypothetical machine and tool. The area below the curve is stable and the area above the curve is unstable. Notice, that at low spindle speeds, due to processing damping effects, large depths of cut can be taken; however, metal removal rate is also low. At higher rotational speed, lobbing exists. This lobbing represents regions of stability at larger depths of cut. Operating within these lobes will produce high levels of metal removal; however, for many materials, this will also result in high tool wear. Therefore, most machines and tools are not designed to operate in this range. Most machines are designed to operate at moderate spindle speeds between n_{min} and n_{max}. For the machine discussed in this paper, it was determined that $n_{min} \approx 700$ r.p.m. and $n_{max} \approx 4000$ r.p.m. per ANSI/ASME standards.

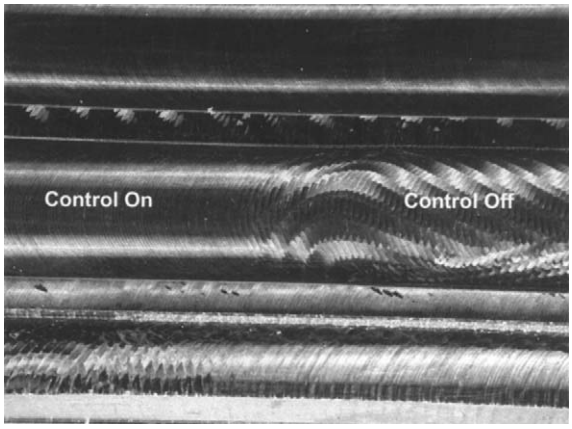

Fig. 10. Enhancement in surface finish.

Cutting instabilities can pump enough vibrational energy into the tool to eject the insert from the part. At ejection, the forces on the tool are relieved and the insert bounces back into the metal. This ejection and reimmersion creates a non-linear dynamic limit cycle process that results in severe vibration in the machine and poor surface finish. The active control system described in this paper absorbed enough energy to significantly alter the onset of this limit cycle. Thereby, it significantly reduced the level of vibration in the machine and enhanced the quality of the finish of a machined component. Fig. 9(a,b) shows the response of the strain gages for a tool in chatter and a tool not in chatter. Notice that chatter can produce over an order of magnitude change in the dynamic response of the tool for a 0.01 mm depth of cut at 3600 r.p.m. spindle speed. Also notice that most of this energy is near the frequency of the tool mode. Fig. 10 shows the surface finish of a cut for the case where control was on and control was off. The quality of the cut was significantly improved by using active control.

As shown in Fig. 11, the stability limit of the machine was also significantly increased due to active control. Per ANSI/ASME standards, chip loading for full immersion cutting was held to 0.1 mm/insert. As shown, an *order of magnitude* increase in the maximum stable depth of cut occurred. Other cutting tests (quarter and half immersion tests) demonstrated improved MMRR with lower levels of performance. For these tests, the maximum stable depth of cut increased by factors of 4 to 5.

6. Conclusions

The work presented in this paper was a validation of the theoretical approach presented in the paper by Dohner et al. [1] in 1997. The experimental results presented show that active structural control could be used to increase the MMRR of a milling machine by up to an order of magnitude. To the authors knowledge this was the first *successful* demonstration of this approach in milling.

Although the above experimental analysis was successful, the design of machines or tool holders that can properly leverage the use of active control is an evolving area of study. These

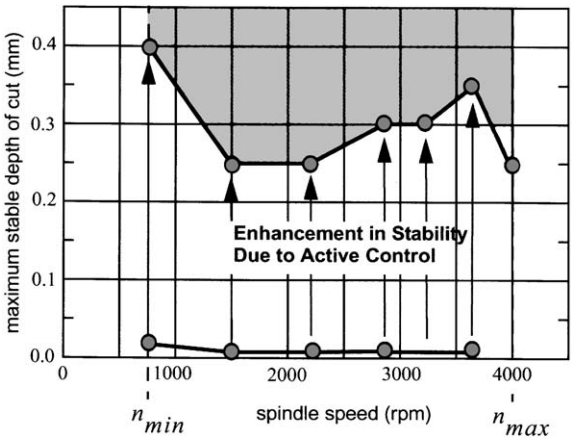

Fig. 11. Enhancement in stability due to active control.

machines and/or components must be designed to allow for the full observability and controllability of the vibration modes of the tool and structure. In the above effort, the tool was altered to overcome this problem, however, in a more mature system, this type of alteration would not be acceptable nor does it appear to be an insurmountable problem to overcome.

Because actuation and sensing occurred in two separate co-ordinate systems, one rotating and the other stationary, the control system was needlessly complex. This complex control system, used in a proof of concept experiment, could be significantly simplified and reduced in cost. In particular, the tool holder approach presented in Ref. [12] could prove to be a very attractive alternative to the present approach. By implementing this approach into a tool holder, the stability of a wide variety of existing machines and tools could be impacted. Moreover, the cost of such a tool holder may not be prohibitive. To determine the applicability of such an adaptation, future research is required.

Active control changes the dynamics of the machine such that chatter instabilities occur at much higher depths of cut. At present, this requires the intervention of an operator. However, theoretically, the machine could be given sufficient intelligence to make these changes on its own. The machine or tool holder could be given the intelligence to sense and adapts its own dynamics to the dynamics of any tool. This gives rise to the concept of smart machines that, with little intervention, can tune their dynamics to the dynamics of a wide variety of tools and materials.

Acknowledgements

The authors would like to thank the following individuals for their support. Dennis Bray (Ingersoll Milling Machine Company), Bob Winfough (Ingersoll), David Martinez (Sandia National Laboratories), Leonard Haynes (IAI), James Handrock, Brian Driessen, Jim Redmond, and Karen Archibeque (Sandia National Laboratories).

Thanks also goes to DARPA for their funding and programmatic guidance, and to the USAF for their efforts as contract managers. Special thanks goes to Lockheed Martin Space Systems Co. for their Request for Loan of Personnel, RFL #99-36.

Appendix A. Matrix values

The plant was realized as a 45th order system by using the eigensystem realization algorithm. This resulted in a balanced realization which was transformed into block diagonal form. Numerical values for the plant are given below. Also given are values for the controller.

$\boldsymbol{A} = 10000^{*}\boldsymbol{a}$, where

$$\boldsymbol{a}(1,1) = -0.0010$$

$$\boldsymbol{a}(2{:}3,2{:}3) = \begin{bmatrix} -0.0045 & 0.0169 \\ -0.0169 & -0.0045 \end{bmatrix}$$

$$\boldsymbol{a}(4{:}5,4{:}5) = \begin{bmatrix} -0.0026 & 0.0244 \\ -0.0244 & -0.0026 \end{bmatrix}$$

$$\boldsymbol{a}(6{:}7,6{:}7) = \begin{bmatrix} -0.0105 & 0.1621 \\ -0.1621 & -0.0105 \end{bmatrix}$$

$$\boldsymbol{a}(8{:}9,8{:}9) = \begin{bmatrix} -0.0064 & 0.1916 \\ -0.1916 & -0.0064 \end{bmatrix}$$

$$\boldsymbol{a}(10{:}11,10{:}11) = \begin{bmatrix} -0.0023 & 0.2831 \\ -0.2831 & -0.0023 \end{bmatrix}$$

$$\boldsymbol{a}(12{:}13,12{:}13) = \begin{bmatrix} -0.0019 & 0.2835 \\ -0.2835 & -0.0019 \end{bmatrix}$$

$$\boldsymbol{a}(14{:}15,14{:}15) = \begin{bmatrix} -0.0112 & 0.3198 \\ -0.3198 & -0.0112 \end{bmatrix}$$

$$\boldsymbol{a}(16{:}17,16{:}17) = \begin{bmatrix} -0.0109 & 0.3246 \\ -0.3246 & -0.0109 \end{bmatrix}$$

$$\boldsymbol{a}(18{:}19,18{:}19) = \begin{bmatrix} -0.0388 & 0.4081 \\ -0.4081 & -0.0388 \end{bmatrix}$$

$$\boldsymbol{a}(20{:}21,20{:}21) = \begin{bmatrix} -0.0278 & 0.4168 \\ -0.4168 & -0.0278 \end{bmatrix}$$

$$\boldsymbol{a}(22{:}23,22{:}23) = \begin{bmatrix} -0.0091 & 0.4926 \\ -0.4926 & -0.0091 \end{bmatrix}$$

$$\boldsymbol{a}(24{:}25,24{:}25) = \begin{bmatrix} -0.0050 & 0.4936 \\ -0.4936 & -0.0050 \end{bmatrix}$$

$$\boldsymbol{a}(26{:}27,26{:}27) = \begin{bmatrix} -0.0967 & 0.05202 \\ -0.5202 & -0.0967 \end{bmatrix}$$

$$\boldsymbol{a}(28{:}29,28{:}29) = \begin{bmatrix} -0.0177 & 0.5526 \\ -0.5526 & -0.0177 \end{bmatrix}$$

$$\boldsymbol{a}(30{:}31,30{:}31) = \begin{bmatrix} -0.0137 & 0.5684 \\ -0.5684 & -0.0137 \end{bmatrix}$$

$$\boldsymbol{a}(32{:}33,32{:}33) = \begin{bmatrix} -0.0961 & 0.7245 \\ -0.7245 & -0.0961 \end{bmatrix}$$

$$\boldsymbol{a}(34{:}35,34{:}35) = \begin{bmatrix} -0.0322 & 0.7438 \\ -0.7438 & -0.0322 \end{bmatrix}$$

$$\boldsymbol{a}(36{:}37,36{:}37) = \begin{bmatrix} -0.1042 & 0.7989 \\ -0.7989 & -0.1042 \end{bmatrix}$$

$$\boldsymbol{a}(38{:}39,38{:}39) = \begin{bmatrix} -0.0160 & 1.0490 \\ -1.0490 & -0.0160 \end{bmatrix}$$

$$\boldsymbol{a}(40{:}41,40{:}41) = \begin{bmatrix} -0.0270 & 1.0808 \\ -1.0808 & -0.0270 \end{bmatrix}$$

$$\boldsymbol{a}(42{:}43,42{:}43) = \begin{bmatrix} -0.0109 & 1.1763 \\ -1.1763 & -0.0109 \end{bmatrix}$$

$$\boldsymbol{a}(44{:}45,44{:}45) = \begin{bmatrix} -0.0123 & 1.1836 \\ -1.1836 & -0.0123 \end{bmatrix}$$

and all other elements of $\boldsymbol{a}$ are zero.

$\boldsymbol{B} = 10000^{*}\boldsymbol{b}$

$$\boldsymbol{b}^{\mathrm{T}}(1{:}2,1{:}8) = \begin{bmatrix} -0.0016 & -0.0160 & 0.0014 & -0.0432 & -0.0270 & 0.0551 & 0.1046 & 0.0175 \\ -0.0047 & -0.0168 & -0.0718 & 0.0449 & 0.0015 & -0.1600 & -0.3317 & -0.0207 \end{bmatrix}$$

$$\boldsymbol{b}^{\mathrm{T}}(1{:}2,9{:}16) = \begin{bmatrix} 0.2978 & 0.0242 & 0.1525 & 0.0397 & -0.0230 & -0.0908 & 0.4576 & 0.0680 \\ 0.1206 & -0.0346 & -0.1174 & 0.0978 & -0.0390 & -0.3136 & 0.0216 & -0.0457 \end{bmatrix}$$

$$\boldsymbol{b}^{\mathrm{T}}(1{:}2,17{:}24) = \begin{bmatrix} -0.2144 & 0.5568 & 0.9123 & 0.0348 & -0.1418 & -0.0995 & 0.0773 & -0.2392 \\ -0.4980 & -0.1732 & 0.0638 & 0.7341 & -0.5774 & 0.1017 & -0.5571 & -0.2313 \end{bmatrix}$$

$$\boldsymbol{b}^{\mathrm{T}}(1{:}2,25{:}32) = \begin{bmatrix} 0.0240 & -0.2842 & -0.1414 & 0.1486 & 0.1603 & 0.4434 & -0.2291 & 0.4508 \\ 0.1612 & 2.2781 & -0.9413 & -0.5878 & -0.4642 & 0.2181 & -0.1195 & 1.1141 \end{bmatrix}$$

$$\boldsymbol{b}^{\mathrm{T}}(1{:}2,33{:}40) = \begin{bmatrix} -2.0570 & -0.2372 & -0.8433 & -0.6595 & 0.2151 & -0.0573 & 0.4518 & 0.0215 \\ -1.2722 & 0.3059 & -0.3928 & 1.5008 & -0.5578 & -0.0028 & 0.0900 & 0.5321 \end{bmatrix}$$

$$
\begin{aligned}
\boldsymbol{b}^{\mathrm{T}}(1{:}2,41{:}45) = {} & -0.1212 \quad 0.2594 \quad 0.1907 \quad -0.0391 \quad 0.124 \\
& 0.4749 \quad 0.4024 \quad -0.2307 \quad 0.3267 \quad -0.5049 \\
\boldsymbol{C}(1{:}2,1{:}8) = {} & -0.0020 \quad -0.0006 \quad 0.0009 \quad 0.0010 \quad -0.0006 \quad 0.0002 \quad -0.0002 \quad 0.0026 \\
& 0.0023 \quad -0.0003 \quad 0.0016 \quad -0.0004 \quad 0.0005 \quad -0.0011 \quad 0.0009 \quad 0.0004 \\
\boldsymbol{C}(1{:}2,9{:}16) = {} & -0.0009 \quad -0.0260 \quad 0.0372 \quad 0.0573 \quad 0.0371 \quad 0.0005 \quad -0.0017 \quad -0.0016 \\
& -0.0002 \quad 0.0239 \quad -0.0258 \quad 0.0716 \quad 0.0334 \quad 0.0006 \quad 0.0013 \quad 0.0010 \\
\boldsymbol{C}(1{:}2,17{:}24) = {} & 0.0009 \quad 0.0019 \quad -0.0121 \quad -0.0038 \quad -0.0026 \quad 0.0001 \quad 0.0020 \quad -0.0015 \\
& 0.0016 \quad -0.0018 \quad 0.0039 \quad -0.0135 \quad 0.0017 \quad -0.0025 \quad -0.0023 \quad 0.0007 \\
\boldsymbol{C}(1{:}2,25{:}32) = {} & 0.0027 \quad 0.0011 \quad -0.0015 \quad 0.0022 \quad -0.0020 \quad -0.0060 \quad -0.0097 \quad 0.0053 \\
& -0.0000 \quad -0.0060 \quad 0.0035 \quad -0.0102 \quad 0.0085 \quad -0.0007 \quad -0.0017 \quad 0.0006 \\
\boldsymbol{C}(1{:}2,33{:}40) = {} & 0.0005 \quad -0.0021 \quad 0.0015 \quad -0.0030 \quad -0.0006 \quad 0.0026 \quad 0.0024 \quad 0.0006 \\
& -0.0002 \quad -0.0000 \quad 0.0003 \quad 0.0038 \quad 0.0025 \quad 0.0003 \quad -0.0001 \quad 0.0024 \\
\boldsymbol{C}(1{:}2,41{:}45) = {} & -0.0002 \quad 0.0032 \quad -0.0010 \quad -0.0010 \quad 0.0013 \\
& -0.0033 \quad 0.0013 \quad 0.0011 \quad -0.0023 \quad -0.0052
\end{aligned}
$$

The controller used to produce Fig. 8 took the form $\Theta(s) = (K_c s + \alpha)/(s^2 + 2\zeta_c \omega_c s + \omega_c^2)$ where $K_c = 7000$, $\alpha = 0.0$, $\zeta_c = 0.4$, $\omega_c = 2\pi\ 290$ rad/s.

References

[1] J.L. Dohner, T.D. Hinnerichs, J.P. Lauffer, C.M. Kwan, M.E. Regelbrugge, N. Shankar, Active chatter control in a milling machine, Proceedings of SPIE, Smart Structures and Materials, Industrial and Commercial Applications of Smart Structures Technologies, March 1997.

[2] H.E. Merritt, Theory of self-excited machine-tool chatter, contribution to machine-tool chatter, research—1, Journal of Engineering for Industry, Transactions of the American Society of Mechanical Engineers 87 (4) (1965) 447–453.

[3] J. Tlusty, F. Ismail, Special aspects of chatter in milling, Journal of Vibration, Acoustics, Stress, and Reliability in Design, Transactions of the American Society of Mechanical Engineers 105 (1983) 24–32.

[4] H.M. Shi, S.A. Tobias, Theory of finite amplitude machine tool instability, International Journal of Machine Tool Design and Research 24 (1) (1984) 45–69.

[5] T. Altintas, P.K. Chan, Process detection and suppression of chatter in milling, International Journal of Machine Tools and Manufacture 32 (3) (1992) 329–347.

[6] CRAC, chatter recognition and control system, US Patent No. 5,170,358, MLI Manufacturing Laboratories, Inc. Gainesville, FL, 1992.

[7] K. Jemielniak, A. Widota, Suppression of self-excited vibration by the spindle speed variation method, International Journal of Machine Tool Design and Research 24 (3) (1984) 207–214.

[8] T.R. Comstock, F.S. Tse, J.R. Lemon, Application of controlled mechanical impedance for reducing machine tool vibrations, Journal of Engineering for Industry, Transactions of the American Society of Mechanical Engineers 91 (4) (1969) 1057–1062.

[9] M.M. Sadek, S.A. Tobias, Reduction of machine tool vibration, American Society of Mechanical Engineering, Applied Mechanics Division, Vol. 1, for meeting, Cincinnati, OH, September 1973, pp. 128–172.

[10] Hong-Yeon Hwang, Jun-Ho Oh, Kwang-Joon Kim, Modeling and adaptive pole assignment control in turning, International Journal of Machine Tool Design and Research 29 (2) (1988) 275–285.

[11] M. Shiraishi, K. Yamanaka, H. Fujita, Optimal control of chatter in turning, International Journal of Machine Tools and Manufacture 31 (1) (1991) 31–43.

[12] Precision machining—active structural control milling concept demonstration system, General Dynamics, Advanced Technology Systems, Guilford Center, Air Force Research Laboratory Report, AFRL-ML-WP-TR-1998-4118, June 1998.

[13] J. Redmond, P. Barney, D. Smith, A biaxial actively damped boring bar for chatter mitigation, The International Journal for Manufacturing Science and Production 2 (1) (1999) 1–16.
[14] Wireless Data Corporation, 620 Clyde Avenue, Mountain View, CA 94043, personal conversations.
[15] H. Kwakernaak, R. Sivan, Linear Optimal Control Systems, Wiley-Interscience, New York, 1972.
[16] Jer-Nan Juang, Applied System Identification, Prentice-Hall, Englewood Cliffs, NJ, 1994.
[17] A.V. Oppenheim, R.W. Schafer, Digital Signal Processing, Prentice-Hall Inc., Englewood Cliffs, NJ, 1975.